Int J Earth Sci (Geol Rundsch) (2017) 106:811–826
DOI 10.1007/s00531-016-1334-z

ORIGINAL PAPER

Early Variscan magmatism along the southern margin of Laurasia: geochemical and geochronological evidence from the Biga Peninsula, NW Turkey

Fırat Şengün[1] · **O. Ersin Koralay**[2]

Received: 21 October 2015 / Accepted: 14 April 2016 / Published online: 5 May 2016

Abstract Massive, fine-grained metavolcanic rocks of the Çamlıca metamorphic unit exposed in the Biga Peninsula, northwestern Anatolia, have provided new Carboniferous ages and arc-related calc-alkaline petrogenesis constraints, suggesting that the Biga Peninsula was possibly involved in the Variscan orogeny. The metavolcanic rocks are mainly composed of metalava and metatuff and have the composition of andesite. Chondrite-normalized REE patterns from these rocks are fractionated (La_N/Yb_N ~ 2.2 to 8.9). Europium anomalies are slightly variable (Eu/Eu* = 0.6 to 0.7) and generally negative (average Eu/Eu* = 0.68). The metavolcanic rocks have a distinct negative Nb anomaly and negative Sr, Hf, Ba, and Zr anomalies. These large negative anomalies indicate crustal involvement in their derivation. Tectonic discrimination diagrams show that all metavolcanic rocks formed within a volcanic arc setting. Zircon ages (LA-ICP-MS) of two samples yield 333.5 ± 2.7 and 334.0 ± 4.8 Ma. These ages are interpreted to be the time of protolith crystallization. This volcanic episode in the Biga Peninsula correlates with other Variscan age and style of magmatism and, by association with a collisional event leading to the amalgamation of tectonic units during the Variscan contractional orogenic event. Carboniferous calc-alkaline magmatism in the Sakarya Zone is ascribed to arc-magmatism as a result of northward subduction of Paleo-Tethys under the Laurasian margin. Geochemical and U–Pb zircon data indicate that the Sakarya Zone is strikingly similar to that of the Armorican terranes in central Europe. The Biga Peninsula shows a connection between the Sakarya Zone and the Armorican terranes.

Keywords Variscan · U–Pb zircon age · Sakarya Zone · Biga Peninsula · Northwest Turkey

Introduction

Anatolia is located in the Eastern Mediterranean region, situated at the interface of the African and Eurasian plates, and records Variscan, Cimmeride, and Alpine orogenic events. The Variscan orogeny, which resulted from the collision between Laurasia and Gondwana, took place during the Carboniferous (e.g., Matte 2001). The Variscan orogeny in Anatolia is either obscured by the intense overprint of the Alpine orogeny or is concealed by younger volcanic events and/or sedimentary cover. The various continental fragments that form Anatolia represent segments from margins of the Paleo-Tethys ocean and isolated continental blocks within this realm (Şengör and Yılmaz 1981; Okay et al. 1996). Each of these continental fragments has distinctive stratigraphic, magmatic, and metamorphic features. The Sakarya Zone in northwestern Anatolia, one of these crustal units, is characterized by Variscan metamorphism–magmatism, Permo-Triassic Paleo-Tethyan accretion–subduction complexes, and clastic products of a Liassic regional unconformity. During the Variscan orogeny, continental and oceanic blocks were accreted to the basement of the Sakarya Zone at the southern margin of Laurasia (e.g., Okay et al. 2006; Okay and Nikishin 2015). The Paleozoic continental basement of the Sakarya Zone, which is well exposed in the Kazdağ and Uludağ Massifs in the west and the Devrekani and Pulur Massifs in the east, is comprised

✉ Fırat Şengün
firatsengun@comu.edu.tr

[1] Department of Geological Engineering, Çanakkale Onsekiz Mart University, 17020 Çanakkale, Turkey

[2] Department of Geological Engineering, Dokuz Eylül University, 35160 İzmir, Turkey

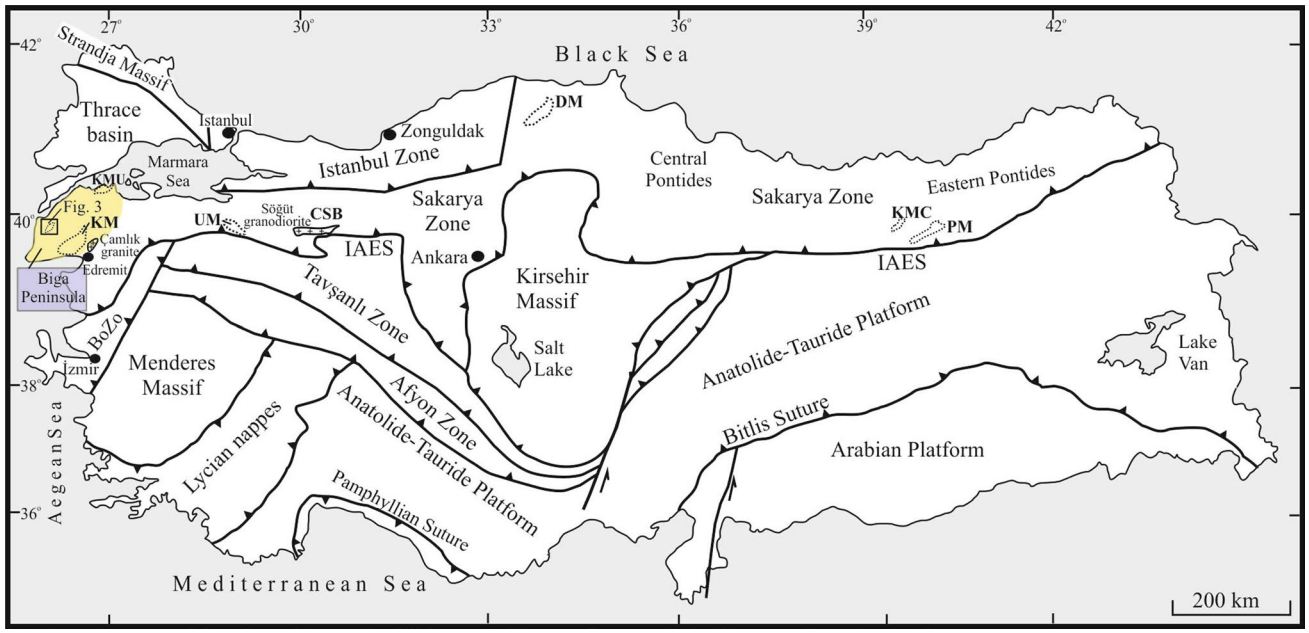

Fig. 1 Tectonic units of Turkey showing major continental blocks and tectonic zones (modified from Okay and Tüysüz 1999; *KMU* Karadağ metamorphic unit, *KM* Kazdağ Massif, *UM* Uludağ Massif, *CSB* Central Sakarya Basement, *DM* Devrakani Massif, *KMC* Kurtoğlu metamorphic complex, *PM* Pulur Massif, *BoZo* Bornova Zone, *IAES* İzmir–Ankara–Erzincan Suture)

of Carboniferous granitic and metamorphic rocks (Okay et al. 1996; Duru et al. 2004; Topuz et al. 2007; Okay et al. 2006, 2008; Ustaömer et al. 2012, 2013). This Carboniferous event in the Sakarya Zone generates a link between the Variscan orogeny in central Europe and the Uralides of Eastern Europe (Okay et al. 2006).

The Paleozoic continental metamorphic rocks of the Biga Peninsula located in the westernmost part of the Sakarya Zone have a complex thermo-tectonic history during the Variscan and Alpine events (Fig. 1; Okay et al. 1996, 2006; Pickett and Robertson 2004; Cavazza et al. 2009). However, Mississippian magmatic activity is not known from the Biga Peninsula. The present study reports Carboniferous protolith ages and tectonic setting of metavolcanic rocks which provide a better understanding of the Variscan orogeny in the Sakarya Zone and demonstrate Armorican affinity of the Sakarya Zone during the Mississippian (Okay et al. 2008; Okay and Nikishin 2015).

Geological framework

The Sakarya Zone in northwestern Anatolia is made up of a tectonic mosaic that includes several tectonic units of continental and oceanic assemblages of different origins and ages. The Biga Peninsula in the Sakarya Zone is bordered to the north by the Strandja Massif and the Thrace Basin, whereas the Aegean Sea marks the western and southern borders (Fig. 1).

The Sakarya Zone

The Sakarya Zone forms an E–W-trending continental sliver that is over 1500 km long and 120 km wide and extends from the Aegean in the west to the Eastern Pontides in the east (Fig. 1). It is bordered by the Strandja Massif and Istanbul Zone to the northwest and by the Black Sea in the northeast. To the south, the Sakarya Zone is in contact with the Taurides and their metamorphic equivalents of Anatolides along the Izmir–Ankara–Erzincan suture zone (Fig. 1). The pre-Jurassic basement of the Sakarya Zone is made up of three different tectonic units (Okay 2008). These are as follows: (1) Variscan basement exposed in the Kazdağ Massif, Çamlıca metamorphic unit, Uludağ Massif, Pulur Massif and Kurtoğlu metamorphic complex dated to the Carboniferous, 330–310 Ma, by zircon and monazite ages (Duru et al. 2004; Okay et al. 2006, 2008; Topuz et al. 2004; 2007; this study); (2) granitoids with Devonian and Permian crystallization ages (Delaloye and Bingöl 2000; Okay et al. 2006; Aysal et al. 2012a, b; Ustaömer et al. 2012; Sunal 2012). Small outcrops of these Paleozoic granitoids are scattered throughout the Sakarya Zone. The Çamlık granodiorite in the Biga Peninsula, one of these Paleozoic granitoids, was dated as Early to Middle Devonian (Aysal et al. 2012a; Okay et al. 1996, 2006); and (3) Permo-Triassic subduction–accretion series of the lower Karakaya Complex (Okay and Göncüoğlu 2004) with Late Triassic blueschist and eclogites (Okay and Monie 1997; Okay et al. 2002) forming part of the Paleo-Tethys oceanic crust that was accreted to

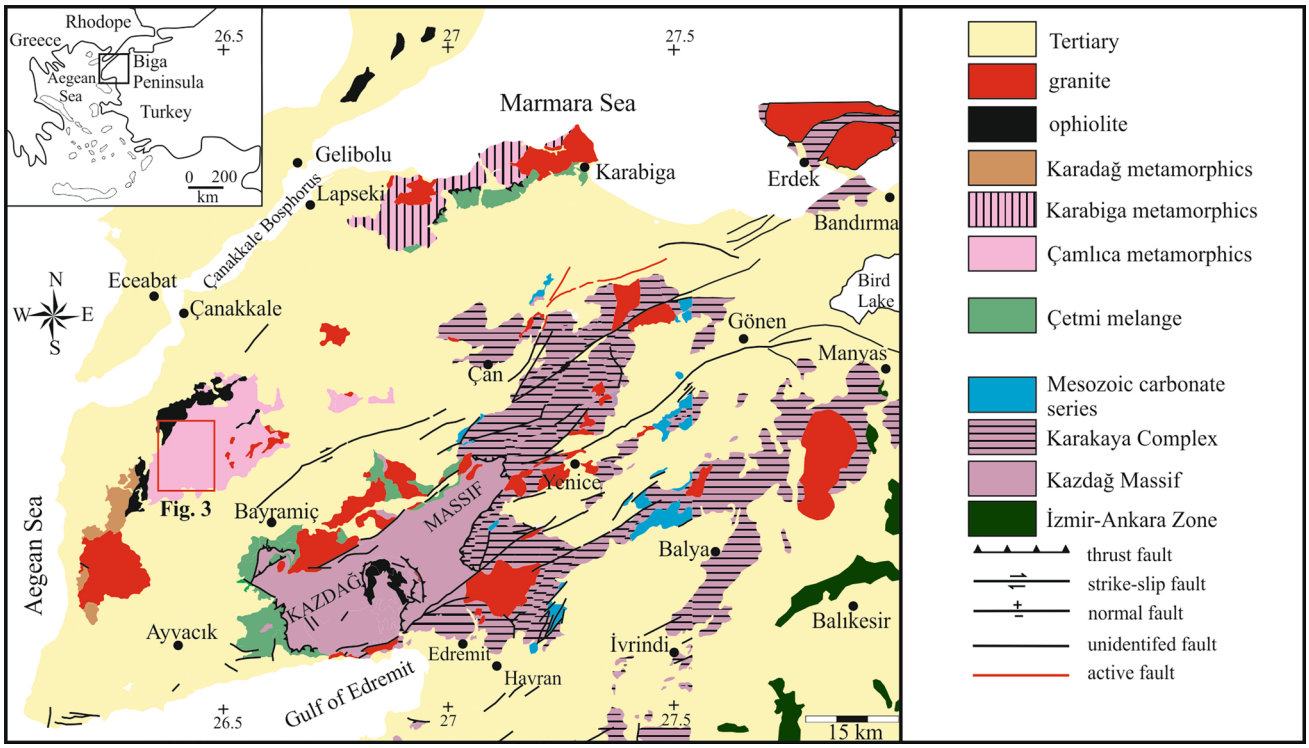

Fig. 2 Generalized geological map of the Biga Peninsula (modified from MTA 2012). *Inset map* shows location of the Biga Peninsula. The *box* indicates the location of the detailed geological map shown in Fig. 3

the southern margin of Laurussia during the Late Permian to Triassic (Stampfli and Kozur 2006; Moix et al. 2008).

A series of strongly deformed clastic and volcanic rocks including exotic blocks of Carboniferous and Permian limestones and radiolarian cherts tectonically lie on the lower Karakaya Complex. The age of these units, called the upper Karakaya Complex, ranges from Permian to Late Triassic (Okay and Göncüoğlu 2004). The basement of the Sakarya Zone is unconformably overlain by a sedimentary and volcanic succession of Early Jurassic age (Altıner et al. 1991). These units are dominated by fluvial to shallow marine carbonate, sandstone, shale, and conglomerate in the western part of Sakarya Zone (Okay 2008).

Carboniferous magmatism is widespread along the Sakarya Zone (Delaloye and Bingöl 2000; Okay et al. 2002, 2006; Topuz et al. 2007, 2010; Dokuz 2011). Most of the plutonic rocks in the basement of the Sakarya Zone are of Carboniferous age ranging between 356 and 303 Ma (Fig. 1). These can be traced from the Kazdağ Massif in the Biga Peninsula (329–308 Ma, Okay et al. 1996, 2006), toward the east (~290 Ma, Okay et al. 2006; 327–319 Ma, Ustaömer et al. 2012) in the Central Pontides (303–275 Ma, Nzegge et al. 2006) and in the Eastern Pontides (324–318 Ma, Topuz et al. 2010; Dokuz 2011). Carboniferous magmatism (356–325 Ma) has also been reported from the Yusufeli area in the eastern Pontides (Ustaömer et al. 2012).

Geology of the Biga Peninsula

The Biga Peninsula is mainly composed of high-grade metamorphic rocks, ophiolites, and plutonic rocks and associated volcanics (Fig. 2). The Peninsula includes the following main rock associations: (1) amphibolite to granulite-facies basement rocks of Kazdağ Massif (Carboniferous; Okay and Satır 2000a, b; Duru et al. 2004; Yaltırak and Okay 2004; Cavazza et al. 2009), and greenschist-facies rocks of the Çamlıca metamorphic unit (Şengün and Çalık 2007; Şengün et al. 2011), and Karabiga metamorphic unit (Late Cretaceous; Beccaletto et al. 2007; Aygül et al. 2012); (2) the Triassic–Early Jurassic units of the Karakaya Complex exposed only in the eastern part of the Biga Peninsula (Okay and Göncüoğlu 2004); (3) the subduction–accretion Çetmi mélange (Early Cretaceous; Okay et al. 1990; Beccaletto et al. 2005); and (4) the Permo-Triassic Karadağ metamorphic unit that is tectonically overlain by the Lower Cretaceous Denizgören ophiolite (Okay et al. 1990; Beccaletto and Jenny 2004). Tertiary sedimentary cover units unconformably overlie all of the units (Fig. 2).

The Çamlıca metamorphic unit is exposed in the westernmost part of the Biga Peninsula and is tectonically imbricated with the Denizgören metaophiolite (Early Cretaceous) to the west. The Denizgören metaophiolite is tectonically

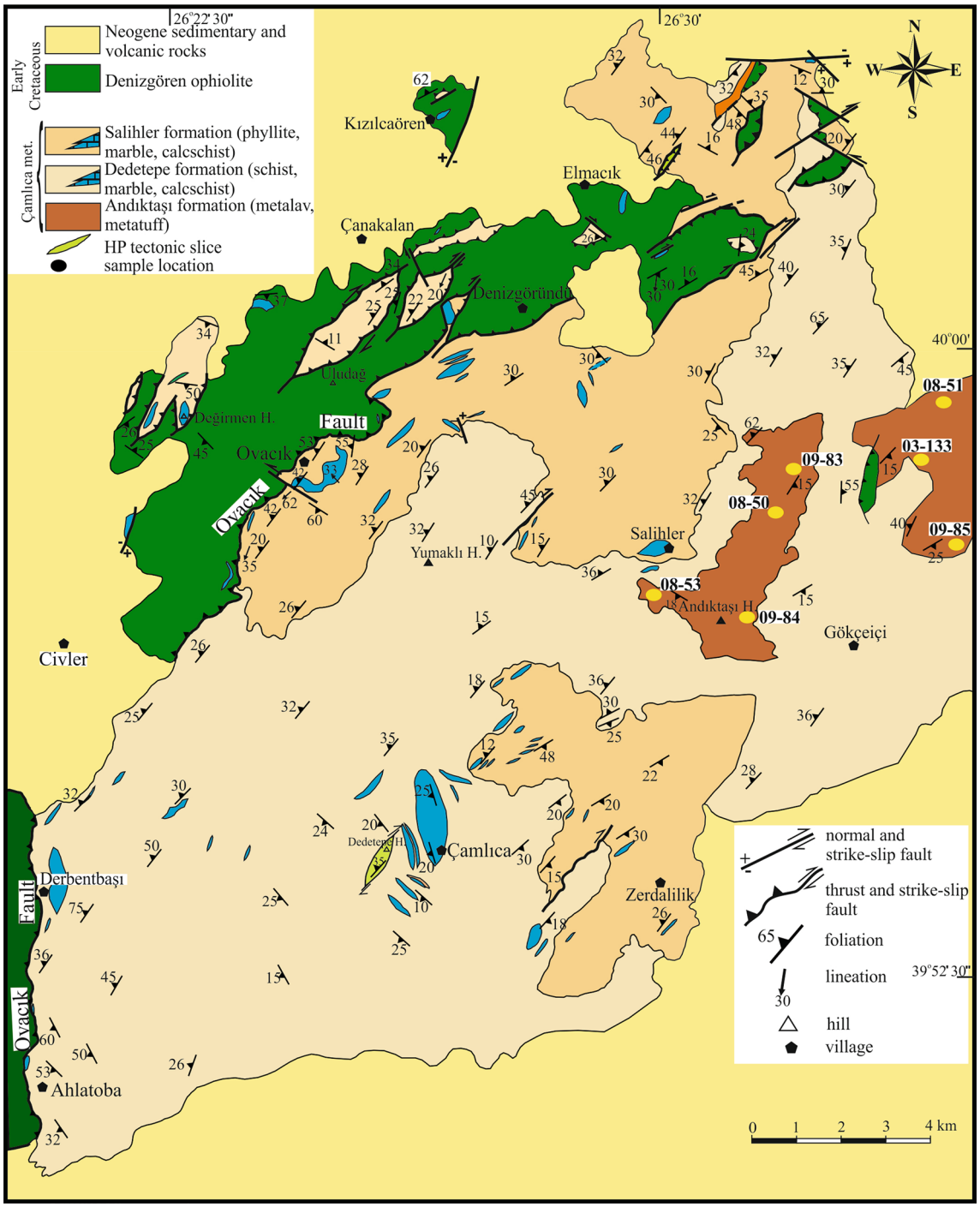

Fig. 3 Geological map of the Çamlıca metamorphic unit. The location of the dated metavolcanic rocks (08–50, 08–51) is shown in the *upper right of the map*

separated from the Çamlıca metamorphic unit by the Ovacık fault (Okay and Satır 2000a), which is 33 km long and forms a broad north to northeast-trending arc (Fig. 3). The Ovacık fault dips west to northwest at 35–40° in the north and 65–70° in the southwest. Southwest of Ovacık village, a mylonitic zone of 1.5 km long and 8–10 m wide represents the Ovacık fault. In this area, lineations plunge 30–60° to the SW. Foliation planes dip 40–50° NW and show a NE–SW trend. Lineation, foliation, and field data suggest that the Ovacık fault is a dextral transpressional strike–slip fault with a reverse component, which caused tectonic slicing. These tectonic slices consist of low-grade metamorphic

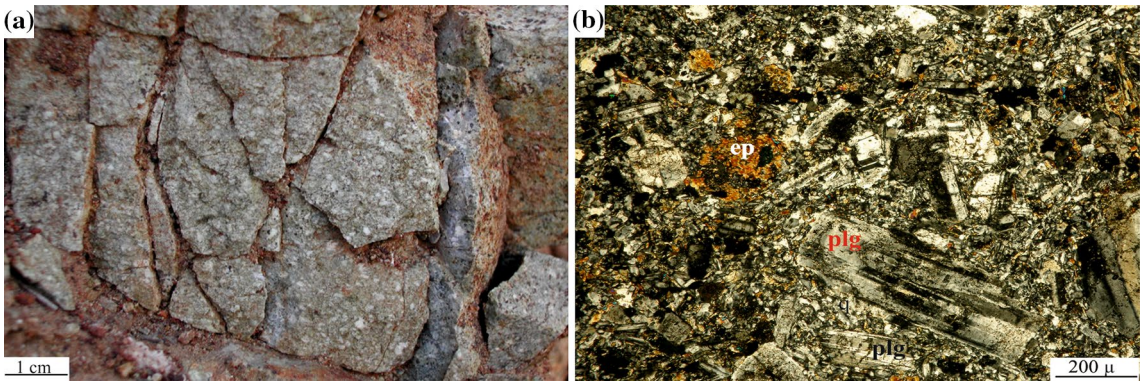

Fig. 4 **a** A close-up view of relic texture reflecting volcanic origin; **b** photomicrograph showing relic volcanic texture

rocks belonging to the Çamlıca metamorphic unit within the Denizgören metaophiolite (Fig. 3). The Çamlıca metamorphic unit is the tectono-stratigraphic basement unit in the Biga Peninsula. This basement has a threefold subdivision: metavolcanic association in the lowermost part (Andıktaşı formation), a metapelitic unit in the upper most part (Salihler formation), and a metapelitic and amphibolitic part (Dedetepe formation) as a transition zone between them (Fig. 3). These three formations completely crop out and are mappable in the Çamlıca metamorphic unit. The metavolcanic association consists of greenschist-facies rocks, predominantly metalavas associated with relatively minor metatuff. This group of rocks has a gradual boundary with the overlying units and exhibits varying degrees of deformation, ranging from massive to weakly schistosed rocks. Eclogite-facies metamorphic rocks occur as tectonic slices within the Dedetepe formation.

Petrography

The metavolcanic rocks exposed in the Çamlıca metamorphic unit are chiefly composed of metalava and metatuff. The mineral assemblage of the metavolcanic rocks is quartz, chlorite, epidote, albite, actinolite, calcite, pyroxene, sphene, and zircon. The metavolcanic rocks are mostly massive and fine-grained rocks. Their primary porphyritic volcanic textures can still be recognized (Fig. 4a, b). Relic primary clinopyroxene is rimmed by epidote, and these phenocrysts are well preserved, probably due to their crystal size (up to 0.6 cm in length). Quartz occurs generally as anhedral crystals and shows undulate extinction. Epidote crystals in metavolcanic rocks are macroscopically clear with yellowish green color and mostly observed as heterogeneously distributed patches. Albite is the most common replacement mineral in metavolcanic rocks and forms coarse porphyroblasts and can occupy as much as 40–50 % of the rock volume. Chlorite is light green and has fibrous texture or forms fringes around existing grains. Actinolite occurs as columnar, bladed, or acicular grains. Calcite, a secondary mineral phase due to alteration, displays deformation twinning. This mineral paragenesis indicates that the metavolcanic rocks experienced lower greenschist-facies metamorphism.

Geochemistry

Analytical methods

Seven representative samples from massive metavolcanics were selected and analyzed for major, trace, and rare earth elements (REE) chemical composition (Fig. 3). Whole-rock analyses were performed by analytical facilities at the ALS Chemex Laboratory in Canada. Major element concentrations were determined by inductively coupled plasma atomic emission spectroscopy (ICP-AES). Trace element and REE concentrations were analyzed by inductively coupled plasma mass spectroscopy (ICP-MS). The prepared sample (0.200 g) was added to lithium metaborate/lithium tetra borate flux (0.90 g), mixed well, and fused in a furnace at 1000 °C. The resulting melt was then cooled and dissolved in 100 mL of 4 % nitric acid 2 % hydrochloric acid. This solution was then analyzed by ICP-AES, and the results were corrected for spectral inter-element interference. The oxide concentration was calculated from the determined elemental concentrations.

Analytical results

Major and trace elements

Major and trace element contents are given in Table 1. The SiO_2 contents of the metavolcanic rocks have a range between intermediate to acidic (62.2–66.3 SiO_2 wt%). The metavolcanic rocks have low to medium Al_2O_3

Table 1 Major and trace element data for the metavolcanic rocks from the Biga Peninsula, NW Turkey

Sample	08–51	08–52	08–53	03–133	09–83	09–84	09–85
Major elements (wt% oxide)							
SiO_2	63.3	64.9	63.6	62.2	66.3	65.6	62.5
Al_2O_3	11.3	8.9	9.8	10.2	11.2	8.0	11.2
Fe_2O_3	3.8	4.8	6.7	6.71	5.8	3.8	5.6
CaO	10.2	15.2	13.2	13.4	11.1	16.1	10.8
MgO	3.1	2.7	2.8	2.8	1.7	2.4	3.2
Na_2O	3.8	0.8	0.8	2.1	1.1	1.3	0.5
K_2O	0.2	0.5	0.1	0.2	0.1	1.9	3.1
TiO_2	0.7	0.5	0.6	0.5	0.6	0.3	0.8
MnO	0.2	0.2	0.3	0.3	0.2	0.2	0.2
P_2O_5	0.1	0.1	0.1	0.1	0.1	0.1	0.1
LOI	1.8	1.2	1.9	1.1	1.5	0.9	1.9
Total	98.8	100	99.4	99.8	100	99.9	100
Trace elements (ppm)							
Ba	42	74.3	9.2	13.6	195	178.5	578
Co	13.5	8	12.8	18.7	6.7	8.6	23.9
Cr	190	40	65	40	200	50	240
Cs	0.6	1.2	4.8	2.2	1.3	1.75	1.5
Cu	71	7	23.9	25.8	59	30	11
Ga	14.7	4.6	12.9	13.4	15.4	5.2	22.7
Hf	3.9	1	2.8	3.6	3.8	1	5.4
Mo	<2	<2	1.7	0.8	<2	<2	<2
Nb	13	8.7	9.7	10.8	11.7	7.9	12
Ni	157	30	31.3	24	112	30	234
Pb	6	10	1	1.1	60	28	40
Rb	5.9	25.4	2.9	3.2	2.3	34.8	138.5
Sn	2	1	2	2	3	1	3
Sr	160.5	165.5	269.7	193.1	317	197	381
Ta	0.9	0.3	0.8	0.7	0.9	0.3	1.4
Th	7.4	2.9	7.2	7.9	8.9	3.7	9.1
Tl	<0.5	<0.5	<0.1	<0.1	0.5	<0.5	<0.5
U	1.4	0.42	1.7	1.5	2.1	0.7	2.4
V	91	22	83	85	89	28	143
W	1	1	0.3	0.6	3	1	2
Y	25.3	20.9	26.8	30	26.9	30.2	37.2
Zn	52	100	6	8	235	147	99
Zr	137	34	104	109	138	34	210

(8–11.3 wt%), low MgO (1–3.2 wt%), low Cr (40–240 ppm), and low Nb (7–13 ppm) contents. The elevated Na_2O (0.5–3.8 wt%) contents in some samples show that they may be altered by low-grade metamorphism. The metavolcanic rocks have higher contents of CaO and P_2O_5. The high relative abundance of CaO ranging from 10.2 to 16.1 wt% is likely to be related to alteration processes as shown by the growth of secondary epidote and calcite.

Trace element characteristics of these metavolcanic rocks reveal that they have calc-alkaline character. Two of these characteristics in particular are important: (1) low contents of incompatible elements (e.g., Nb, Y, Zr) and low Nb/Y ratios (Pearce 1996), and (2) low Cr (up to 240 ppm), V (22–91 ppm), and Ni (<160 ppm) concentrations (Table 1). Most metavolcanic samples cluster in the field of andesite (Fig. 5a). The Th/Yb versus Ta/Yb plot including the MORB (mid-ocean ridge basalt) and OIB (ocean island basalt) array separates depleted mantle (MORB) and enriched mantle (intraplate) sources (Fig. 5b; Pearce 1982). All metavolcanic rocks with higher Th values were probably derived from an enriched mantle source, modified by the addition of a subduction component (Fig. 5b). The Th/

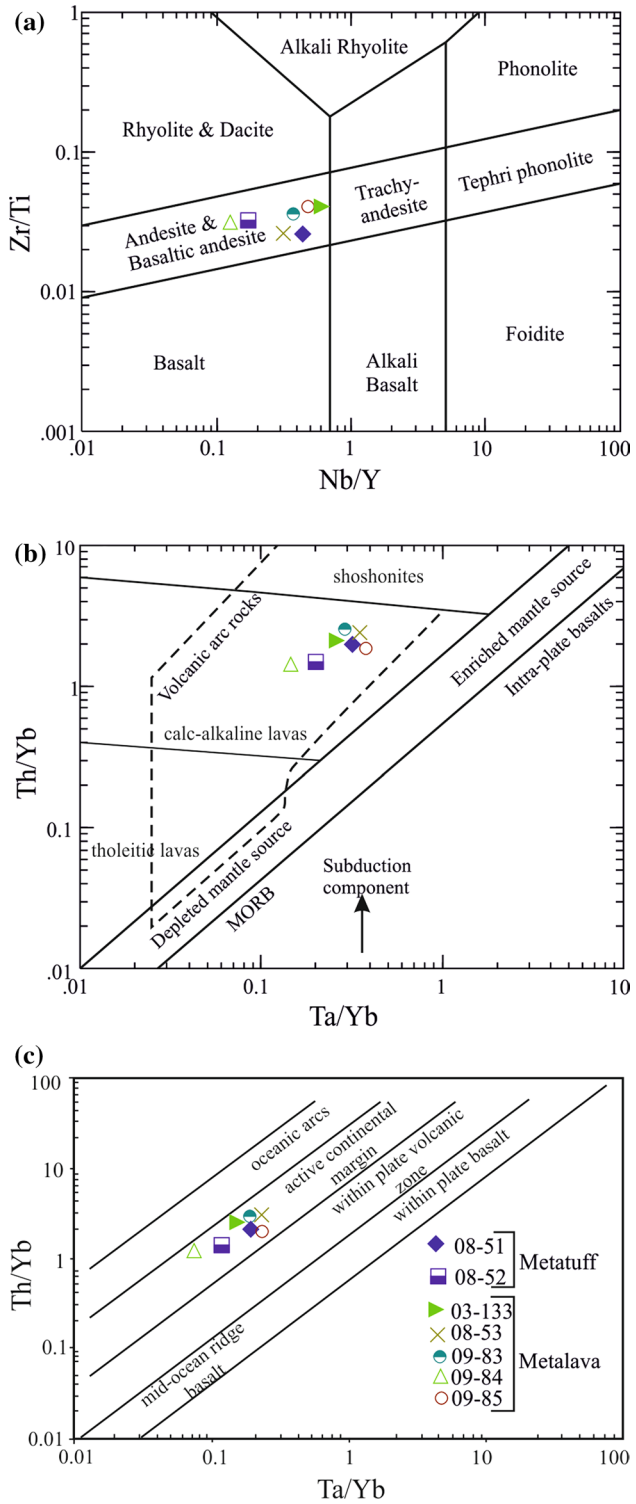

Fig. 5 **a** Rock classification diagram of metavolcanic rocks from the Biga Peninsula (after Pearce 1996). **b** Th/Yb versus Ta/Yb diagram (after Pearce 1982) showing source characteristics for the metavolcanic rocks. **c** Th/Yb versus Ta/Yb geodynamic setting discrimination diagram of Pearce (1983) modified by Gorton and Schandl (2000)

Yb versus Ta/Yb diagram (Pearce 1983 modified by Gorton and Schandl 2000) shows that most metavolcanic rocks cluster in the active continental margin field (Fig. 5c).

The N-type MORB-normalized multi-element spider diagram for metavolcanic rocks is shown in Fig. 6a. The metavolcanic rocks have a distinct negative Nb and Ta anomaly, typically seen in arc magmas, with negative Sr, Ba, Hf anomalies (Fig. 6a). The low field-strength (LFS) elements are mobile in aqueous fluids, so hydration that accompanies greenschist-facies metamorphism may have affected their concentrations. Rubidium, in particular, shows a wide scatter in values. Most Th and Ce abundances are enriched compared to neighboring elements (Fig. 6a). Thorium abundances vary considerably between samples, and high Th/Nb ratios are seen in many samples (03–133, 08–51, 08–53, 09–83, and 09–85). These features also indicate either a subduction signature or crustal contamination (Stern et al. 1995; Pearce 1996). All the samples of metavolcanic rocks display large ion lithophile element (LILE) enrichment and depletions in high field-strength elements (HFSE), especially for Nb (Fig. 6a). Depletion of HFSE is stated to be controlled by their immobility during the melting of the mantle peridotite in a subduction zone (McDonough 1991).

Rare earth elements (REE) are known to be the least mobile elements during hydrothermal alteration and low-grade metamorphism (Michard 1989; Peate 1997). Therefore, the chondrite-normalized REE diagrams give valuable insight into the source of magmas and their crystallization evolution. Chondrite-normalized REE diagrams illustrate that the metavolcanic rocks from the Biga Peninsula generally exhibit LREE enrichment with respect to HREE (Table 2; Fig. 6b). All the samples have similar flat heavy rare earth element (HREE) patterns (Gd_N/Yb_N ~ 1.6 to 2.4). Chondrite-normalized REE patterns are moderately fractionated (La_N/Yb_N ~ 2.2 to 8.9). Europium anomalies are slightly variable (Eu/Eu* = 0.6 to 0.7) and generally negative (average Eu/Eu* = 0.68). Europium anomalies are mainly controlled by the presence or fractionation of feldspar. Thus, the removal of feldspar from the melt by crystal fractionation or the partial melting of a rock causes a negative Eu anomaly in the melt (Rollinson 1993). The plagioclase fractionation may be confirmed by the slight development of a negative Eu anomaly (Fig. 6b).

Tectonic and genetic constrains

The large negative Nb, Sr, Ba, and Zr anomalies in the metavolcanic rocks suggest crustal involvement in their derivation as indicated by the multi-element diagram

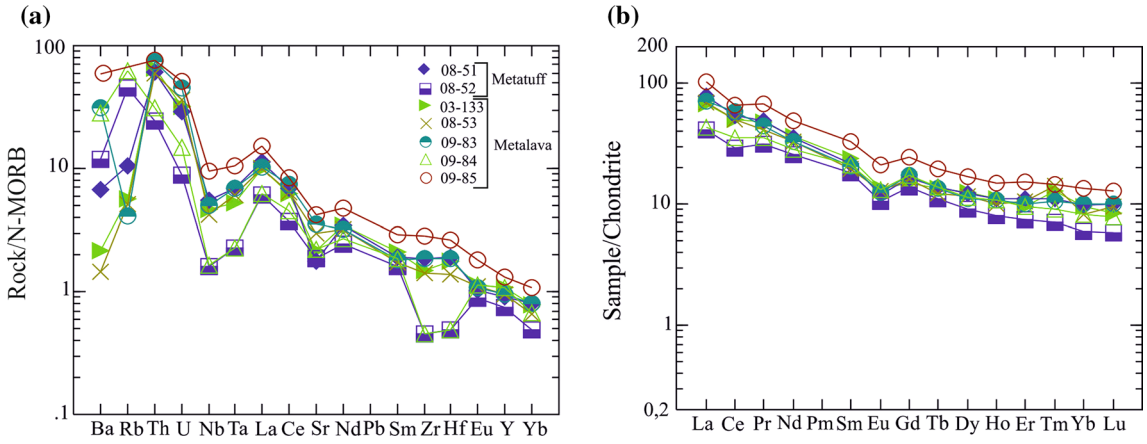

Fig. 6 **a** N-type MORB-normalized (normalization values are from Sun and McDonough 1989), and **b** Chondrite-normalized REE patterns of the metavolcanic rocks. Chondrite normalizing values from Taylor and McLennan (1985)

Table 2 REE data analyzed by ICP-MS for metavolcanic rocks from the Biga Peninsula, NW Turkey

Sample	08–51	08–52	08–53	03–133	09–83	09–84	09–85
Rare earth elements (ppm)							
La	28.5	15.1	25.2	24.7	25.8	15.8	37.8
Ce	51.9	27.8	47.5	47.3	56.1	33.8	67.5
Pr	6.6	4.2	5.7	6.4	6.1	4.8	9.2
Nd	25.3	18	23.5	25.5	23.4	19.9	34.5
Sm	5	4.2	4.5	5.5	4.8	4.9	7.6
Eu	1	0.9	1.1	1.2	1.1	1.1	1.8
Gd	5.1	4.2	4.8	4.6	5.3	5.3	7.5
Tb	0.8	0.6	0.7	0.9	0.9	0.8	1.1
Dy	4.6	3.5	4.4	4.8	4.2	4.3	6.4
Ho	0.9	0.7	0.9	0.9	0.9	0.9	1.3
Er	2.7	1.8	2.6	2.4	2.5	2.4	3.8
Tm	0.4	0.2	0.5	0.5	0.4	0.3	0.5
Yb	2.4	1.5	2	2.4	2.5	2.1	3.3
Lu	0.4	0.2	0.4	0.3	0.4	0.3	0.5
Gd_N/Yb_N	1.7	2.4	2	1.6	1.8	2.1	1.9
La_N/Yb_N	8.3	7.3	8.9	8.4	7.5	5.5	8.2
Eu/Eu*	0.6	0.7	0.7	0.7	0.7	0.7	0.7

(Fig. 6a). The crustal influence may be related to either partial melting of the base of continental crust or contamination of mafic magma with crustal material. Th enrichment relative to Nb is a distinctive feature of ocean floor and back-arc basalts (Saunders and Tarney 1979; Wilson 1989). Distinctive negative Nb anomalies in many intermediate to basic rocks are commonly attributed to a subduction component (Brique et al. 1984; Green 1995; West et al. 2004). This subduction component can be incorporated into magmas erupted in fore-arc, back-arc, or intra-arc regions above a subduction zone. In the multi-element diagram (Fig. 6a) normalized to N-type MORB values of Sun and McDonough (1989), trace element data show that the rocks possess a typical calc-alkaline volcanic arc trace element pattern.

The tectono-magmatic setting of the metavolcanic rocks has been determined by several discrimination diagrams using relatively immobile trace elements. Plotting the immobile elements that preserve their abundance through post-formational processes in a Zr versus Y diagram (Müller et al. 2001), all the samples show arc-related affinity (Fig. 7a). The tectonic setting of the metavolcanic rocks is a volcanic arc (Fig. 7b), as indicated by the Th–Hf–Ta ternary discrimination diagram (Wood 1980). Those within the VAB (volcanic arc basalts) are distributed below the line defined by Hf/Th = 3 indicating calc-alkaline magma

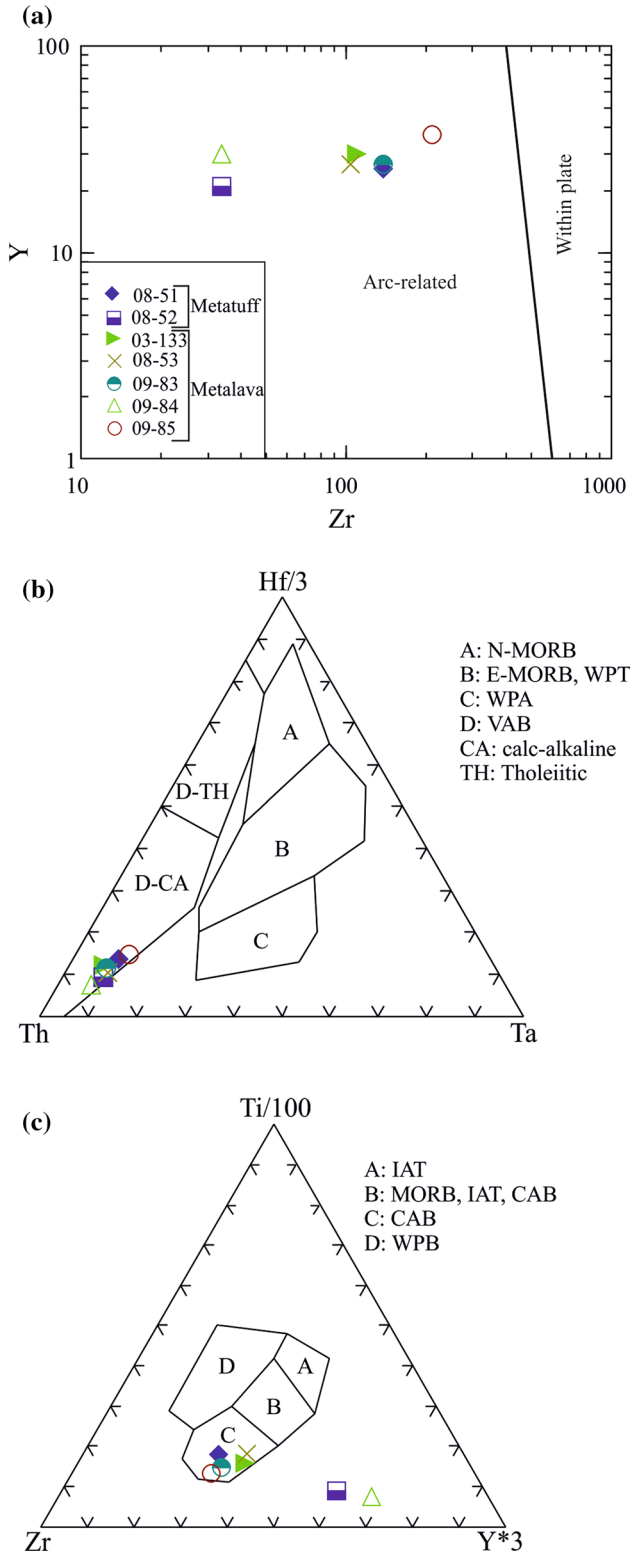

Fig. 7 Tectonic discrimination diagrams of the metavolcanic rocks. Diagrams after **a** Müller et al. (2001); **b** Wood (1980); **c** Pearce and Cann (1973). *IAT* island-arc tholeiite, *MORB* mid-ocean ridge basalt, *CAB* calc-alkali basalt, *WPB* within-plate basalt, *WPT* within-plate tholeiite, *WPA* within-plate alkali, *VAB* volcanic arc basalt

type. Data plotted in the Ti–Zr–Y ternary discrimination diagram (Pearce and Cann 1973) is consistent with a volcanic arc tectonic setting (Fig. 7c). The majority of the samples, with the exception of two (08–52, 09–84), plot in the field of calc-alkaline basalt (Fig. 7c).

Geochronology

Sample preparation and analytical procedures

Zircons were separated from crushed whole-rock weighing 15–20 kg each, to obtain a substantial amount of representative grains. Zircons were separated at the Department of Geology Engineering, Dokuz Eylül University. Zircon fractions were isolated by standard procedures using magnetic separation, heavy liquids and, finally, hand-picking for analysis under a binocular microscope. Zircon grains were mounted in epoxy resin and polished to expose the grain centers. Photomicrographs were taken to identify the exact spots for laser ablation analysis and prepared for orientation using reflected light in the laser ablation sample cell. To identify different zircon growth zones, CL imaging was carried out with a microprobe CAMECA SX51 in the Institute of Geology and Geophysics, Chinese Academy of Sciences, Beijing (IGG, CAS).

U–Pb zircon age determinations were performed by laser ablation ICP-MS at University of Science and Technology of China in Hefei, using an ArF excimer laser system (GeoLas Pro, 193-nm wavelength) and a quadrupole ICP-MS (PerkinElmer Elan DRCII). The analyses were carried out with a pulse rate of 10 Hz, beam energy of 10 J/cm^2, and a spot diameter of 44 μm, sometimes 32 and 60 μm when necessary. The detailed analytical procedure is similar to Yuan et al. (2004). Uncertainties in isotope ratios are quoted at the 1σ level, and uncertainties in ages are reported at the 95 % confidence level. Standard zircon 91500 was analyzed to calibrate the mass discrimination and elemental fractionation, the U/Pb ratios were processed using a macro program LaDating@Zrn written in Excel™ spreadsheet software. Common Pb was corrected by ComPb corr#3-18 (Andersen 2002). Ages and diagrams were generated using the Isoplot/Ex 3.75 software package of Ludwig (2012).

Sample description

Zircons from two metavolcanic rocks (Andıktaşı formation), samples 08–50 (39°58′19″N–26°31′46″E) and 08–51 (39°59′17″N-26°33′34″E) (Fig. 3), were dated to reveal the primary crystallization age of the metavolcanic rocks in the basement of the Çamlıca metamorphic unit. Samples 08–50

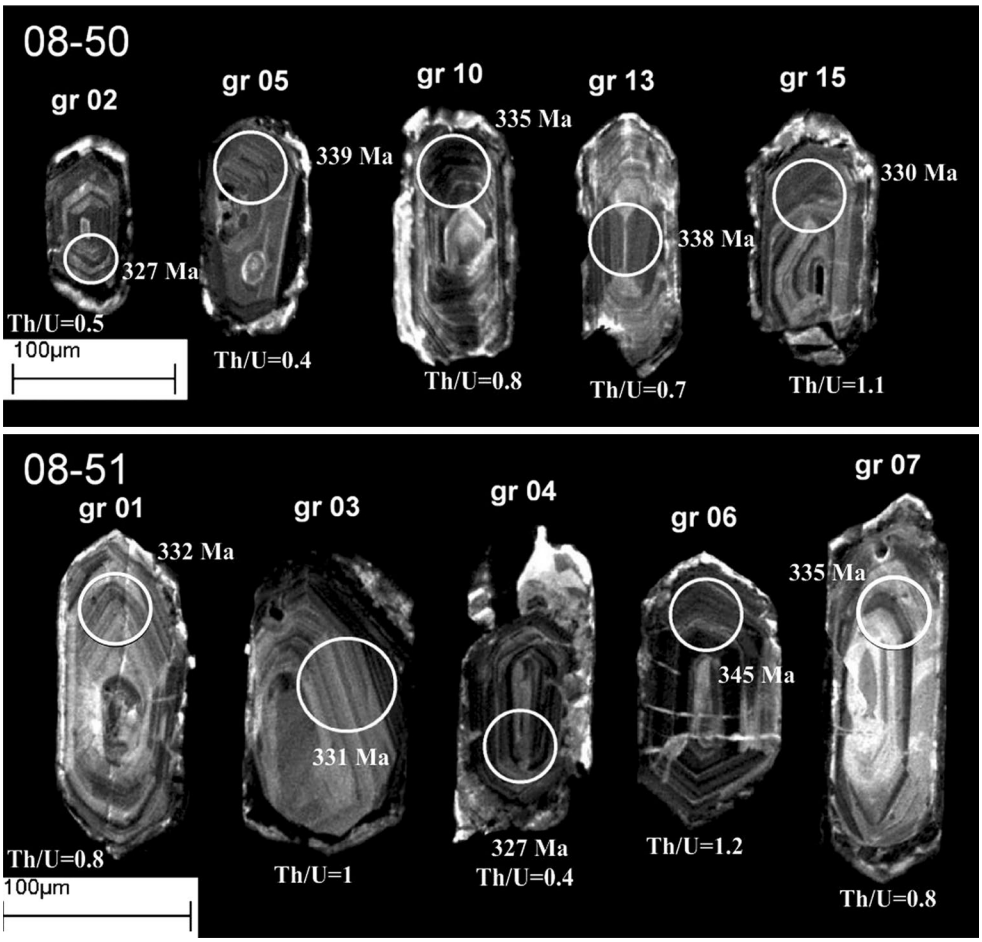

Fig. 8 Cathodoluminescence (CL) images of selected zircons from metavolcanic samples (08–50 and 08–51). Spots on zircons represent areas of LA-ICP-MS analyses

and 08–51 consist mainly of quartz, chlorite, epidote, albite, actinolite, and calcite. The main accessory minerals are zircon, sphene, and opaque minerals. The zircon grains in sample 08–50 are predominantly colorless, translucent, and short prismatic with generally 2:1, rarely 3:1, length/width ratios. The internal structure of the zircons, revealed by CL imaging, shows typical oscillatory zoning for the magmatic zircons (Fig. 8). Some crystals contain large cores showing relics of original growth banding of magmatic origin. Zircons are euhedral and have pitted surfaces. They show brighter rims reflecting metamorphism effects. Zircons separated from sample 08–51 are similar in morphology, with a predominance of colorless, translucent, and short prismatic with generally 3:1, rarely 2:1, length/width ratios. Most of these zircons are predominantly euhedral and show oscillatory zoned internal structures indicating a magmatic origin (Fig. 8). The zircon grains shown in Fig. 8 indicate normal cores preserving oscillatory zoning of magmatic origin; however, evidence for old ages indicates the presence of xenocrystic core material.

Analytical results

Eighteen spot analyses from sample 08–50 and 14 from 08 to 51 were performed. Corrected isotope data and ages are presented in Table 3. The zircons used for age calculations from sample 08–50 have U contents of 184–685 ppm and Th/U ratio ranging from 0.4 to 1.4 with an average of 0.9, indicating typical magmatic origin. The main zircon population spreads along the concordia curve from 300 to 350 Ma (Fig. 9a). All concordant data between 90 and 110 % concordance yield a weighted average $^{206}Pb/^{238}U$ age estimate of 333.5 ± 2.7 Ma (n = 14, MSWD = 0.99, 95 % conf.). The TuffZirc algorithm for a coherent group of fourteen analyses generates 334.5 ± 3.5 Ma. In addition, three analyses cluster around ~640 Ma. This suggests that the oldest spot ages are affected by mixing of xenocryst core material or existence of inherited zircons. One grain (grain 8) yields relatively young age of 309.0 ± 4.0 Ma and was not used for age calculations. Most probably, it reflects loss of radiogenic Pb by a later thermal event. The

Table 3 Laser ablation ICP-MS U–Pb data and calculated ages for zircons from metavolcanic samples (08–50 and 08–51)

Sample	Th	U	Th/U	Isotopic ratios						Ages						6/8/7/5 conc. %
				$^{207}Pb/^{206}Pb$	1σ	$^{207}Pb/^{235}U$	1σ	$^{206}Pb/^{238}U$	1σ	$^{207}Pb/^{206}Pb$	1σ	$^{207}Pb/^{235}U$	1σ	$^{206}Pb/^{238}U$	1σ	
08–50																
gr 01	95	184	0.5	0.16112	0.01210	0.43222	0.04445	0.05310	0.00153	2467	136	365	32	334	9	92
gr 02	254	245	1.0	0.05148	0.00378	0.38022	0.02951	0.05378	0.00115	262	138	327	22	338	7	103
gr 03	456	623	0.7	0.05652	0.00404	0.40521	0.03053	0.05295	0.00087	473	139	345	22	333	5	97
gr 04[a]	325	456	0.7	0.06312	0.00441	0.92874	0.06992	0.10677	0.00173	712	134	667	37	654	10	98
gr 05	136	305	0.4	0.05330	0.00361	0.39491	0.02834	0.05399	0.00084	341	135	338	21	339	5	100
gr 06[a]	1154	1387	0.8	0.07024	0.00469	1.00853	0.07198	0.10479	0.00155	936	123	708	36	642	9	91
gr 07	396	568	0.7	0.05565	0.00538	0.41037	0.04415	0.05435	0.00090	438	212	349	32	341	6	98
gr 08[a]	48	201	0.2	0.05796	0.00387	0.39075	0.02785	0.04910	0.00062	528	136	335	20	309	4	92
gr 09	185	295	0.6	0.05964	0.00429	0.42907	0.03315	0.05244	0.00077	591	144	363	24	329	5	91
gr 10	446	551	0.8	0.05492	0.00368	0.40170	0.02869	0.05337	0.00073	409	137	343	21	335	4	98
gr 11	882	642	1.4	0.05419	0.00373	0.39960	0.02965	0.05359	0.00086	379	139	341	22	337	5	99
gr 12	1556	1889	0.8	0.05548	0.00406	0.41599	0.03183	0.05450	0.00099	432	139	353	23	342	6	97
gr 13	335	465	0.7	0.04975	0.00448	0.38452	0.03320	0.05384	0.00112	184	156	330	24	338	7	102
gr 14[a]	2154	1921	1.1	0.06597	0.00444	0.92599	0.06618	0.10256	0.00150	805	126	666	35	629	9	94
gr 15	763	685	1.1	0.05672	0.00388	0.40918	0.02956	0.05257	0.00073	481	137	348	21	330	4	95
gr 16	452	364	1.2	0.05103	0.00449	0.37064	0.03292	0.05229	0.00097	242	166	320	24	329	6	103
gr 17	337	342	1.0	0.05026	0.00449	0.37660	0.03298	0.05305	0.00098	207	163	325	24	333	6	102
gr 18	259	337	0.8	0.05847	0.00414	0.41372	0.03147	0.05164	0.00073	548	143	352	23	325	4	92
08–51																
gr 01	183	217	0.8	0.05106	0.00390	0.36979	0.02955	0.05278	0.00094	243	148	320	22	332	6	104
gr 02[a]	276	1229	0.2	0.06698	0.00542	0.51803	0.04858	0.05588	0.00087	837	172	424	32	350	5	83
gr 03	477	468	1.0	0.05233	0.00353	0.37820	0.02718	0.05276	0.00074	300	139	326	20	331	5	102
gr 04	258	617	0.4	0.05129	0.00351	0.36462	0.02673	0.05197	0.00070	254	142	316	20	327	4	103
gr 05	336	284	1.2	0.05971	0.00481	0.44435	0.03718	0.05465	0.00100	593	151	373	26	343	6	92
gr 06	553	456	1.2	0.05680	0.00388	0.43102	0.03113	0.05491	0.00075	484	137	364	22	345	5	95
gr 07	389	473	0.8	0.05865	0.00408	0.43005	0.03185	0.05333	0.00096	554	131	363	23	335	6	92
gr 08[a]	224	411	0.5	0.06625	0.00452	0.77939	0.05668	0.08588	0.00118	814	130	585	32	531	7	91
gr 09	114	126	0.9	0.05876	0.00410	0.42486	0.03177	0.05253	0.00072	558	141	360	23	330	4	92
gr 10[a]	1886	2354	0.8	0.12689	0.00835	4.77956	0.33861	0.27395	0.00402	2055	105	1781	59	1561	20	88
gr 11[a]	1245	1327	0.9	0.18333	0.02077	0.70736	0.07631	0.02903	0.00074	2683	146	543	45	184	5	34
gr 12	254	477	0.5	0.05712	0.00397	0.41939	0.03079	0.05360	0.00078	496	137	356	22	337	5	95
gr 13[a]	886	785	1.1	0.07158	0.00472	0.99648	0.07011	0.10164	0.00144	974	121	702	36	624	8	89
gr 14	224	244	0.9	0.05732	0.00412	0.42752	0.03240	0.05333	0.00111	504	131	361	23	335	7	93

[a] Analyses not used in age calculation

weighted average age of 333.5 ± 2.7 Ma can be interpreted as the primary crystallization age of this metavolcanic rock.

The zircons used for age calculations from sample 08–51 have U contents of 126–617 ppm and Th/U ratio ranging from 0.4 to 1.2 with an average of 0.8, indicating typical magmatic origin. From 14 analyzed zircons in sample 08–51, nine analyzes cluster around 330 Ma on the concordia diagram (Fig. 9b). All concordant data between 90 and 110 % concordance yield a weighted average $^{206}Pb/^{238}U$ age estimate of 334.0 ± 4.8 Ma ($n = 9$, MSWD = 1.5, 95 % conf.). Similarly, TuffZirc age yields 335.0 (+8, −5) Ma on a group of nine analyses. Five grains display older ages, between 530 and 2055 Ma, representing the existence of inherited components. The weighted average age of 334.0 ± 4.8 Ma is interpreted to represent primary crystallization age of the volcanic protolith.

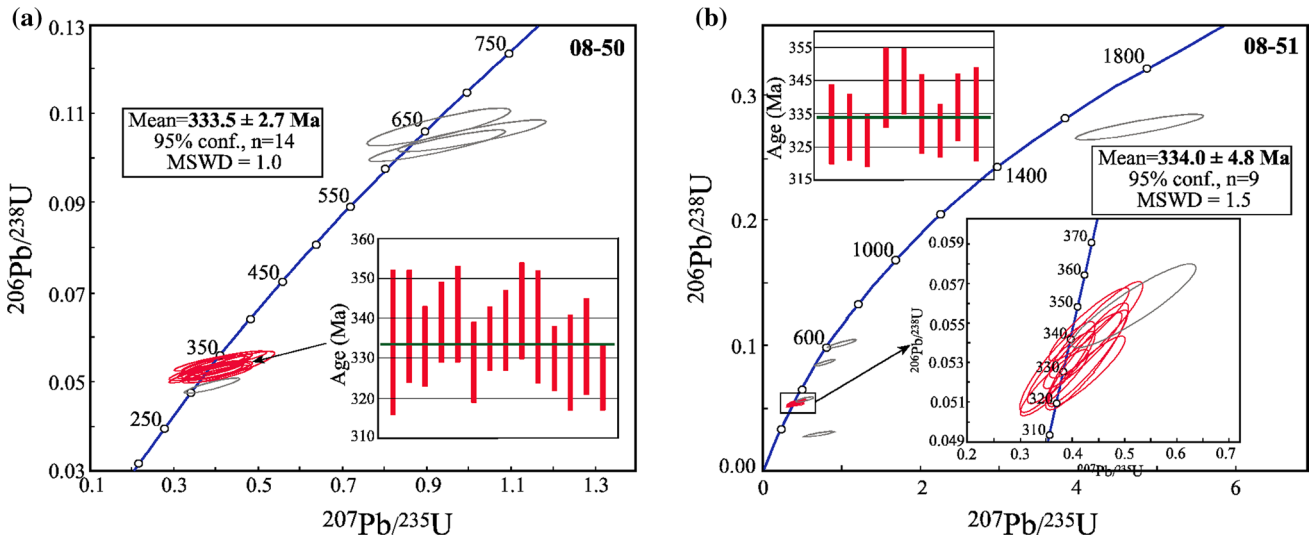

Fig. 9 Concordia diagrams showing U–Pb isotope ratios and ages derived from LA-ICP-MS analyses for metavolcanic samples **a** 08–50 and **b** 08–51

Discussion

Variscan magmatism in the Sakarya Zone

The Carboniferous accretion of the Sakarya Zone to the Laurasian margin resulted in intense deformation, Carboniferous metamorphism, and magmatism (Okay et al. 2006). The age of Variscan magmatism in the Sakarya Zone ranges from 298 to 285 Ma (Ar–Ar biotite plateau ages and K–Ar biotite ages, respectively, Delaloye and Bingöl 2000; Okay et al. 2002). However, U–Pb zircon ages from the Söğüt granodiorite cutting the Central Sakarya basement are Mississippian (Fig. 1; 319–327 Ma; Ustaömer et al. 2012). The age of magmatism in the eastern Pontides (Pulur Massif, Kurtoğlu metamorphic complex) has also been dated as Mississippian (324–318 Ma; Topuz et al. 2010; Dokuz 2011). Mississippian magmatism (356–325 Ma) has also been reported from the Yusufeli area in the eastern Pontides (Ustaömer et al. 2012). However, Mississippian magmatic activity has not been documented in the Biga Peninsula yet. Zircons from two metavolcanic rocks (this study) yielded ages of 333.5 ± 2.7 and 334.0 ± 4.8 Ma (Mississippian). These ages are interpreted as the time of protolith crystallization of the metavolcanics. This volcanic episode in the Biga Peninsula coincides well with the Variscan magmatic activity observed overall in the Sakarya Zone and a subduction event leading to the amalgamation of tectonic units during the Variscan orogenic event. A similar tectonic scenario can be envisaged for Çamlıca metavolcanics. In previous studies, magmatic activity occurred in the latest Pennsylvanian to Early Permian period, probably linked to crustal thickening (Okay et al. 2006; Okay 2008). These ages from metavolcanics in the Biga Peninsula show that this magmatic activity relating to the Variscan orogeny prevailed during Mississippian in the Sakarya Zone. However, all metavolcanic rocks from the Çamlıca metamorphic unit formed within a volcanic arc setting characterized by calc-alkaline magma type. Variscan magmatism in the Central Pontides (Nzegge et al. 2006; Ustaömer et al. 2012) and in the Eastern Pontides (Topuz et al. 2010; Dokuz 2011) is generally characterized by calc-alkaline, intermediate to basic rocks, which is ascribed to arc-magmatism during the closure of the Paleo-Tethys ocean (Topuz et al. 2010; Dokuz 2011; Ustaömer et al. 2013).

Variscan orogeny: subduction of Paleo-Tethys under Laurasia

The Variscan orogeny comprises Carboniferous to Early Permian deformation, metamorphism, and magmatism ascribed to the collision and amalgamation of Gondwana, Laurasia, and intervening terranes (Matte 2001; Warr 2002; von Raumer et al. 2003; von Raumer et al. 2009; Stampfli et al. 2011) in southern Europe, southeastern North Africa, northwestern Africa, which resulted in the creation of supercontinent Pangaea (e.g., Ziegler 1989; Stampfli et al. 2013). Paleozoic evolution of the eastern Mediterranean was marked by the opening and closure of ocean basins and continental crust formation in the accompanying subduction zones (e.g., Stampfli et al. 2001; Stampfli and Borel 2002).

Neoproterozoic and Early Paleozoic Gondwana-derived blocks assembled after the Silurian and subsequently accreted to the Laurasian margin during the Variscan

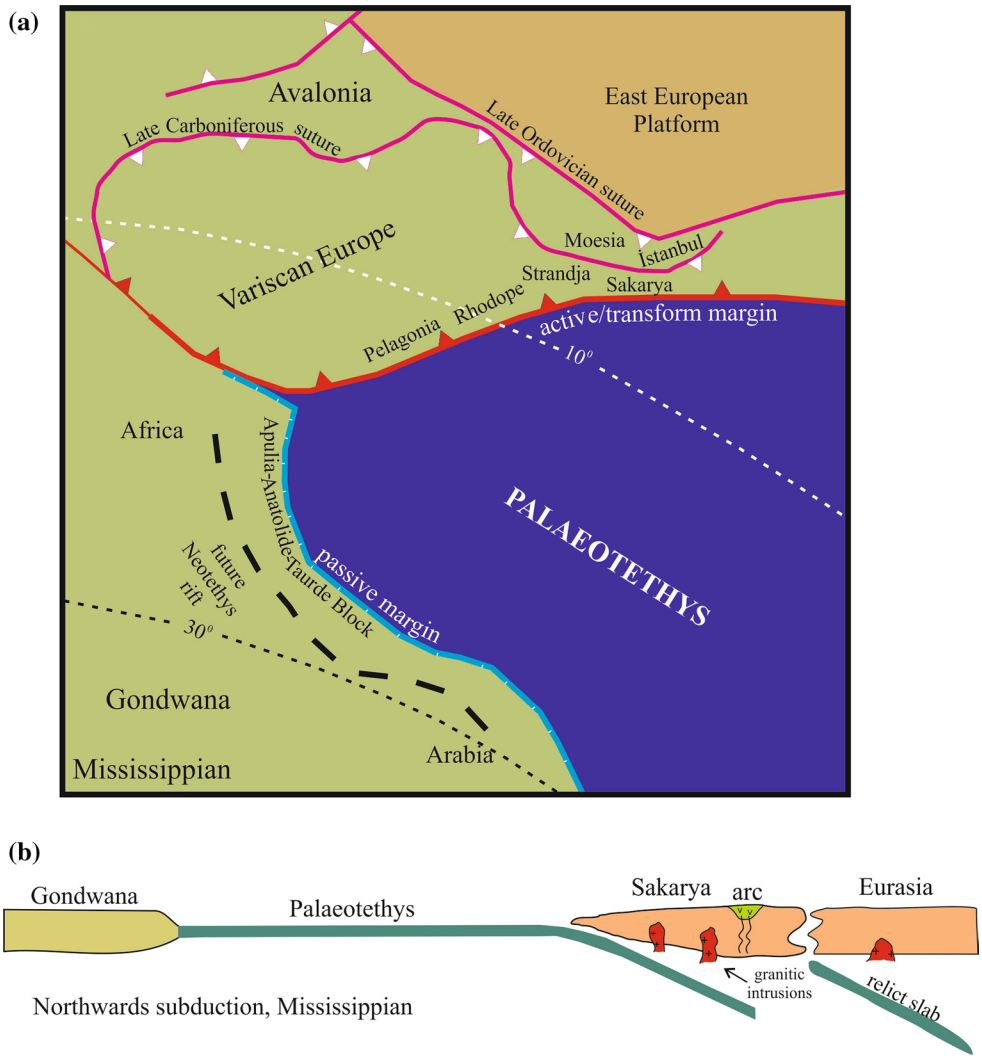

Fig. 10 **a** Paleogeographic reconstruction of the eastern Mediterranean region for the Mississippian (modified after Stampfli and Borel 2002; Okay et al. 2006). Paleo-Tethys separated Eurasia from Gondwana and subducted northward beneath the Eurasia during the Mississippian time. However, the northern margin of Gondwana remained passive. **b** Tectonic model for Turkey during the Carboniferous Variscan orogeny. Mississippian magmatism can be attributed to subduction. The Sakarya Zone in the northwest Turkey and other continental fragments rifted from Gondwana during early Paleozoic time and then drifted northwards till they accreted to the active continental margin of Eurasia (modified from Stampfli and Borel 2002)

orogeny in Mississippian times (von Raumer et al. 2003; Stampfli and Borel 2002; von Raumer and Stampfli 2008). Accretion of Gondwana-derived blocks to Laurasia was followed by the opening of the Paleo-Tethys. The opening of Paleo-Tethys (Stampfli and Borel 2002; Stampfli and Kozur 2006; von Raumer et al. 2009) caused further fragmentation of the northern Gondwana margin, with the formation of a narrow continental magmatic arc. This magmatic arc refers to a microcontinent or group of continental fragments that rifted away from Gondwana toward the end of the Silurian and collided with Laurasia (Baltica, Laurentia, Avalonia, and Armorica) toward the end of the Carboniferous during the Variscan orogeny (Fig. 10a, b; von Raumer et al. 2009; Stampfli and Kozur 2006; Stampfli et al. 2011; Okay and Nikishin 2015). This arc comprises the Rhodope and Strandja Massifs in the Balkans, the Sakarya Zone in the Pontides and the Caucasus, which can be correlated with the Armorican terranes in central Europe (Fig. 10a). In this continental magmatic arc, the Armorican terrane is the outermost unit and also the first unit to collide with terranes derived from Laurasia (Hanseatic terrane, Stampfli and Borel 2002). The Armorican terranes are generally characterized by calc-alkaline, intermediate to basic chemistry, and exhibit a significant mantle contribution (Shaw et al. 1993; Pin and Paquette 2002). Units located in the inner side of the arc contain the intra-alpine and Mediterranean terranes characterized by Carboniferous or early Permian arc type magmatism (Stampfli et al. 2011). This Carboniferous calc-alkaline magmatism corresponds to the continuing subduction of Paleo-Tethys under the southern margin of Laurasia and subsequent Gondwana–Laurasia collision (Stampfli and Borel 2002; Zanchi et al. 2003; Stampfli et al. 2011).

Implications for regional geology

The Sakarya Zone forms an elongate crustal ribbon extending from the Aegean in the west to the Eastern Pontides in

the east. The Çamlıca metamorphic unit occurs in the westernmost part of the Sakarya Zone. The Variscan evolution of the Sakarya Zone may be similar to that of the Balkans, Pelagonian Zone, Rhodope Massif, and central Europe in terms of Carboniferous magmatism, metamorphism, and geological evolution. The Variscan plutonism in Bulgaria and in northern Turkey is Mississippian–Early Permian in age (320–270 Ma) (Okay et al. 2001, 2002, Carrigan et al. 2005; Sunal et al. 2006, 2008; Topuz et al. 2007, 2010; Anders et al. 2007; Ustaömer et al. 2012). However, magmatism in the Biga Peninsula is slightly older (~335 Ma) compared to Bulgaria, northern Turkey, and the Pelagonian Zone.

Carboniferous magmatism is common throughout the Pelagonian Zone (e.g., Anders et al. 2007). Magmatic age of Carboniferous basement rocks in the Pelagonian Zone ranges from 320 to 307 Ma (Vavassis et al. 2000; De Bono 1998), which indicates subduction-zone magmatism. The Pelagonian Zone and other continental fragments, notably the Sakarya Zone, split from Gondwana during the early Paleozoic and then drifted northward till they accreted to the opposite, active continental margin of Laurasia (Fig. 10b; Stampfli et al. 2001; Stampfli and Kozur 2006; Robertson 2012). Thus, Carboniferous magmatic rocks as remnants of a magmatic arc on the southern margin of Laurasia resulted from northward subduction of Paleo-Tethys Ocean.

The Variscan orogenic belt in central Europe marks the continental collision zone between Laurussia to the north and Gondwana to the south (Dewey and Burke 1973; Matte 1991). Variscan Massifs in Europe (e.g., the Bohemian Massif, Armorica, Black Forest Massif, French Massif Central, Alpine basements, Moesia) record Carboniferous plutonism and deformation (Linnemann et al. 2004; Carrigan et al. 2005; Ballèvre et al. 2009 and references therein). During the Mississippian, rocks with monzodioritic to quartzdioritic composition are described in the European Variscides, which were typically emplaced syntectonically between 340 and 330 Ma (Debon and Lemmet 1999) along major dextral strike–slip faults.

Conclusions

Zircons from two metavolcanic samples yielded ages of 333.5 ± 2.7 and 334.0 ± 4.8 Ma (Mississippian). They can be interpreted as the time of protolith crystallization of metavolcanics. Carboniferous metavolcanic rocks occur in the Sakarya Zone located on the northern of the İzmir–Ankara suture and are the products of subduction-related magmatism. The Carboniferous calc-alkaline magmatism in the Sakarya Zone resulted from northward subduction of the Paleo-Tethys under the southern margin of Laurasia. These metavolcanics from the Çamlıca metamorphic unit are connected with an arc which developed on the continental crust at the subduction-related active continental margin, which is characterized by calc-alkaline magma. This magmatic arc comprises the Sakarya Zone in the Pontides, the Rhodope and Strandja Massifs in the Balkans, and the Caucasus which can be correlated with the Armorican terranes in central Europe. The Biga Peninsula shows a connection between the Sakarya Zone and the Armorican terranes.

Acknowledgments This study was supported by the Scientific and Technological Research Council of Turkey (TÜBİTAK) Grant 110Y281. We are grateful to Osman Candan for his valuable suggestions on an earlier version of this manuscript. Constructive reviews by Pierre Barbey and Philippe Rossi helped to clarify the picture and considerably improved the manuscript.

References

Altıner D, Koçyiğit A, Farrinaci A, Nicosa U, Conti MA (1991) Jurassic–Lower Cretaceous stratigraphy of the southern part of northwestern Anatolia (Turkey). Geol Romanna 27:13–30

Anders B, Reischmann T, Kostopoulos D (2007) Zircon geochronology of basement rocks from the Pelagonian Zone, Greece: constraints on the pre-Alpine evolution of the westernmost internal Hellenides. Int J Earth Sci 96:639–661

Andersen T (2002) Correction of common lead in U–Pb analyses that do not report ^{204}Pb. Chem Geol 192:59–79

Aygül M, Topuz G, Okay AI, Satır M, Meyer HP (2012) The kemer metamorphic complex (NW Turkey), a subducted continental margin of the Sakarya Zone. Turk J Earth Sci 21:19–35

Aysal N, Ustaömer T, Öngen S, Keskin M, Köksal S, Peytcheva I, Fanning M (2012a) Origin of the Early-Middle Devonian magmatism in the Sakarya Zone, NW Turkey: geochronology, geochemistry and isotope systematics. J Asian Earth Sci 45:201–222

Aysal N, Öngen S, Peytcheva I, Keskin M (2012b) Origin and evolution of the Havran Unit, Western Sakarya basement (NW Turkey): new LA-ICP-MS U-Pb dating of the metasedimentary–metagranitic rocks and possible affiliation to Avalonian microcontinent. Geodin Acta 25(3–4):226–247

Ballèvre M, Bosse V, Ducassou C, Pitra P (2009) Palaeozoic history of the Armorican Massif: models for the tectonic evolution of the suture zones. C R Geosci 341:174–201

Beccaletto L, Jenny C (2004) Geology and correlation of the Ezine Zone: a Rhodope fragment in NW Turkey? Turk J Earth Sci 13:145–176

Beccaletto L, Bartolini AC, Martini R, Hochuli PA, Kozur H (2005) Biostratigraphic data from Çetmi Melange, northwest Turkey: palaeogeographic and tectonic implications. Palaeogeogr Palaeoclimatol Palaeoecol 221:215–244

Beccaletto L, Bonev N, Bosch D, Bruguier O (2007) Record of a Palaeogene syn-collisional extension in the north Aegean Sea: evidence from the Kemer micaschists (NW Turkey). Geol Mag 144:393–400

Brique L, Bougault H, Joron JL (1984) Quantification of Nb, Ta, Ti and V anomalies in magmas associated with subduction zones: petrogenetic implications. Earth Planet Sci Lett 68:257–263

Carrigan CW, Mukasa SB, Haydoutov I, Kolcheva K (2005) Age of Variscan magmatism from the Balkan sector of the orogen, central Bulgaria. Lithos 82:125–147

Cavazza W, Okay AI, Zattin M (2009) Rapid early-middle Exhumation of the Kazdağ Massif (western Anatolia). Int J Earth Sci 98:1935–1947

De Bono A (1998) Pelagonian Margins in central Evia island (Greece): stratigraphy and geodynamic evolution. Dissertation, Universite de Lausanne

Debon F, Lemmet M (1999) Evolution of Mg/Fe ratios in late Variscan plutonic rocks from the external crystalline massifs of the Alps (France, Italy, Switzerland). J Petrol 40:1151–1185

Delaloye M, Bingöl E (2000) Granitoids from western and northwestern Anatolia: geochemistry and modeling of geodynamic evolution. Int Geol Rev 42:241–268

Dokuz A (2011) A slab detachment and delamination model for the generation of Carboniferous high-potassium I-type magmatism in the Eastern Pontides, NE Turkey: the Kose composite pluton. Gondwana Res 19:926–944

Duru M, Pehlivan Ş, Şentürk Y, Yavaş F, Kar H (2004) New results on the lithostratigraphy of the Kazdağ Massif in northwest Turkey. Turk J Earth Sci 13:177–186

Gorton MP, Schandl ES (2000) From continents to island arcs: a geochemical index of tectonic setting for arc-related and within plate felsic to intermediate volcanic rocks. Can Miner 38:1065–1073

Green TH (1995) Significance of Nb/Ta as an indicator of geochemical processes in the crust-mantle system. Chem Geol 120:347–359

Linnemann U, McNaughton NJ, Romer RL, Gehmlich M, Drost K, Tonk C (2004) West African provenance for Saxo-Thuringia (Bohemian Massif): did Armorica ever leave pre-Pangean Gondwana? U–Pb-SHRIMP zircon evidence and the Nd-isotopic record. Int J Earth Sci 93:683–705

Ludwig KR (2012) User's manual for Isoplot 3.75 a geochronological toolkit for Microsoft Excel. Berkeley Geochronology Center Special Publication No. 5, USA

Matte P (1991) Accretionary history of the Variscan belt in western Europe. Tectonophysics 43:109–125

Matte P (2001) The Variscan collage and orogeny (480–290 Ma) and the tectonic definition of the Armorican microplate: a review. Terra Nova 13:122–128

McDonough WF (1991) Partial melting of subducted oceanic crust and isolation of its residual eclogitic lithology. Philos Trans R Soc Lond 335A:407–418

Michard A (1989) Rare earth element systematic in hydrothermal fluids. Geochim Cosmochim Acta 53:745–750

Moix P, Beccaletto L, Kozur H, Hochard C, Rosselet F, Stampfli GM (2008) A new classification of the Turkish terranes and sutures and its implication for the paleotectonic history of the région. Tectonophysics 451:7–39

MTA (2012) General and economic geology of the Biga Peninsula. Special Publication Series 28, 326 p. (in Turkish)

Müller D, Franz L, Herzig PM, Hunt S (2001) Potassic igneous rocks from the vicinity of epithermal gold mineralization, Lihir Island, Papua New Guinea. Lithos 75:163–186

Nzegge OM, Satır M, Siebel W, Taubald H (2006) Geochemical and isotopic constraints on the genesis of the Late Palaeozoic Deliktaş and Sivrikaya granites from the Kastamonu granitoid belt (Central Pontides, Turkey). Neues Jb Miner Abh 183:27–40

Okay AI (2008) Geology of Turkey: a synopsis. Anschnitt 21:19–42

Okay AI, Göncüoğlu MC (2004) The Karakaya complex: A Review of data and concepts. Turk J Earth Sci 13:77–95

Okay AI, Monie P (1997) Early Mesozoic subduction in the Eastern Mediterranean: evidence from Triassic eclogite in northwest Turkey. Geology 25:595–598

Okay AI, Nikishin AM (2015) Tectonic evolution of the southern margin of Laurasia in the Black Sea region. Int Geol Rev 57(5–8):1051–1076

Okay AI, Satır M (2000a) Upper Cretaceous eclogite-Facies metamorphic rocks from the Biga Peninsula, Northwest Turkey. Turk J Earth Sci 9:47–56

Okay AI, Satır M (2000b) Coeval plutonism and metamorphism in a latest Oligocene metamorphic core complex in Northwest Turkey. Geol Mag 137:495–516

Okay AI, Tüysüz O (1999) Tethyan sutures of northern Turkey. In: Durand B, Jolivet L, Horvath F, Seranne M (eds) The Mediterranean basins: tertiary extension within the Alpine orogen, vol 156. Geological Society, London, pp 475–515

Okay AI, Siyako M, Bürkan KA (1990) Biga Yarımadası'nın Jeolojisi ve Tektonik Evrimi. Turk Assoc Pet Geol Bull 2(1):83–121

Okay AI, Satır M, Maluski H, Siyako M, Monie P, Metzger R, Akyüz S (1996) Paleo-and Neotethyan events in northwest Turkey. In: Yin A, Harrison M (eds) Tectonics of Asia. Cambridge University Press, Cambridge, pp 420–441

Okay AI, Satır M, Tüysüz O, Akyüz S, Chen F (2001) The tectonics of the Strandja Massif: Variscan and mid-Mesozoic deformation and metamorphism in the northern Aegean. Int J Earth Sci 90:217–233

Okay AI, Monod O, Monie P (2002) Triassic blueschists and eclogites from northwest Turkey: vestiges of the Paleo-Tethyan subduction. Lithos 64:155–178

Okay AI, Satır M, Siebel W (2006) Pre-Alpide and Mesozoic orogenic events in the Eastern Mediterranean region. Geol Soc Lond Mem 32:389–405

Okay AI, Bozkurt E, Satır M, Yiğitbaş E, Crowley QG, Shang CK (2008) Defining the southern margin of Avalonia in the Pontides: geochronological data from the Late Proterozoic and Ordovician granitoids from NW Turkey. Tectonophysics 461:252–264

Pearce JA (1982) Trace element characteristics of lavas from destructive plate boundaries. In: Thorpe RS (ed) Andesites. Wiley, New York, pp 525–548

Pearce JA (1983) Role of sub-continental lithosphere in magma series at active continental margins. In: Hawkesworth CJ, Norry MJ (eds) Continental basalts and mantle xenolith. Shiva Publications, Cheshire, pp 230–249

Pearce JA (1996) A user's guide to basalts discrimination diagrams. In: Wyman DA (ed) Trace element geochemistry of volcanic rocks: applications for massive sulfide exploration. Short course notes 12. Geol Asso Can, pp 79–113

Pearce JA, Cann JR (1973) Tectonic setting of basic volcanic rocks determined using trace element analysis. Earth Planet Sci Lett 19:290–300

Peate DW (1997) The Parana-Etendeka province. In: Mahoney J, Coffin M (eds) Large igneous provinces: continental, oceanic, and planetary flood volcanism. Geoph Monog Series, Washington, pp 217–245

Pickett EA, Robertson AHF (2004) Significance of the volcanogenic Nilüfer unit and related components of the Triassic Karakaya Complex for Tethyan subduction/accretion processes in NW Turkey. Turk J Earth Sci 13:97–143

Pin C, Paquette JL (2002) Le magmatisme basique calcoalcalin d'age dévono-dinantien du nord du Masif Central, témoin d'une merge active hercynienne: arguments géochimiques et isotopiques Sr:Nd. Geodin Acta 15:63–77

Robertson AHF (2012) Late Palaezoic–Cenozoic tectonic development of Greece and Albania in the context of alternative reconstructions of Tethys in the Eastern Mediterranean region. Int Geol Rev 54(4):373–454

Rollinson H (1993) Using geochemical data: evaluation, presentation, interpretation. Longman Geochemistry Series, Harlow

Saunders AD, Tarney J (1979) The geochemistry of basalts from a back-arc spreading center in the Scotia Sea. Geochim Cosmochim Acta 43:55–72

Şengör AMC, Yılmaz Y (1981) Tethyan evolution of Turkey: a plate tectonic approach. Tectonophysics 75:181–241

Şengün F, Çalık A (2007) Çamlıca Metamorfitlerinin (Biga Yarımadası, KB Türkiye) Metamorfizma Özellikleri ve Korelasyonu. Geol Bull Turkey 50:1–16

Şengün F, Yigitbas E, Tunç İO (2011) Geology and tectonic emplacement of eclogite and blueschist, Biga Peninsula, Northwest Turkey. Turk J Earth Sci 20:273–285

Shaw A, Downes H, Thirlwall MF (1993) The quartz-diorites of Limousin: elemental and isotopic evidence for Deveno–Carboniferous subduction in the Hercynian belt of the French Massif Central. Chem Geol 107:1–18

Stampfli GM, Borel GD (2002) A plate tectonic model fort he Paleozoic and Mesozoic constrained by dynamic plate boundaries and restored synthetic oceanic isochrones. Earth Planet Sci Lett 196:17–33

Stampfli GM, Kozur H (2006) Europe from the Variscan to the Alpine cycles. In: Gee DG, Stephenson R (eds) European lithosphere dynamics, vol 32. Geol Soc Lond Memoirs, London, pp 57–82

Stampfli GM, Mosar J, Faure P, Pillevuit A, Vannay JC (2001) Permo-Mesozoic evolution of the western Tethys realm: the Neotethys/East-Mediterranean connection. In: Ziegler PA, Cavazza W, Robertson AHF, Crasquin-Soleau S (eds) Peri-Tethys Memoir, 6:Peritethyan rift/wrench basins and passive margins, Mémoire Musée National Histoire Naturelle 186, pp 51–108

Stampfli GM, von Raumer J, Wilhem C (2011) The distribution of Gondwana derived terranes in the early paleozoic, in: Gutiérrez-Marco JC, Rábano I, García-Bellido D (eds) Ordovician of the World. Cuadernos del Museo Geominero, 14. Instituto Geológico y Minero de España, Madrid, pp 567–574

Stampfli GM, Hochard C, Verard C, Wilhem C, vonRaumer J (2013) The formation of Pangea. Tectonophysics 593:1–19

Stern RA, Syme EC, Lucas SB (1995) Geochemistry of 1.9 Ga MORB- and OIB-like basalts from Amisk collage, Flin Flon belt, Canada: evidence for an intra-oceanic origin. Geochim Cosmochim Acta 59:3131–3154

Sun SS, McDonough WF (1989) Chemical and isotopic systematics of oceanic basalts: implications for mantle composition and processes. In: Saunders AD, Norry MJ (eds) Magmatism in the ocean basins, vol 42. Geol Soc Lond, London, pp 313–345

Sunal G (2012) Devonian magmatism in the western Sakarya Zone, Karacabey region, NW Turkey. Geodin Acta 25(3–4):183–201

Sunal G, Satır M, Natal'in BA, Toraman E (2006) Paleozoic magmatic events in the Strandja Masif. Geodin Acta 19(5):283–300

Sunal G, Satır M, Natal'in BA, Toraman E (2008) Paleotectonic position of the Strandja massif and surrounding continental blocks based on zircon Pb–Pb age studies. Int Geol Rev 50:519–545

Taylor SR, McLennan SM (1985) The continental crust: its composition and evolution. Blackwell Scientific, Oxford

Topuz G, Altherr R, Kalt A, Satır M, Werner O, Schwarz WH (2004) Aluminous granulites from the Pulur complex, NE Turkey: a case of partial melting, efficient melt extraction and crystallization. Lithos 72:183–207

Topuz G, Altherr R, Schwarz WH, Dokuz A, Meyer H (2007) Variscan Amphibolite-facies rocks from the Kurtoğlu metamorphic complex (Gümüşhane Area, Eastern Pontides, Turkey). Int J Earth Sci 96:861–873

Topuz G, Altherr R, Siebel W, Schwarz WH, Zack T, Hasözbek A, Barth M, Satır M, Şen C (2010) Carboniferous high-potassium I-type granitoid magmatism in the Eastern Pontides: the Gümüşhane pluton (NE Turkey). Lithos 116:92–110

Ustaömer PA, Ustaömer T, Robertson AHR (2012) Ion Probe U–Pb dating of the Central Sakarya basement: a peri-Gondwana terrane intruded by late Lower Carboniferous subduction/collision-related granitic rocks. Turk J Earth Sci 21:905–932

Ustaömer T, Robertson AHR, Ustaömer PA, Gerdes A, Peytcheva I (2013) Constraints on Variscan and Cimmerian magmatism and metamorphism in the Pontides (Yusufeli–Artvin area), NE Turkey from U–Pb dating and granite geochemistry. In: Robertson AHF, Parlak O, Ünlügenç UC (eds) Geological development of Anatolia and the easternmost Mediterranean region, vol 372. Geol Soc Lond, London, pp 49–74

Vavassis I, De Bono A, Stampfli G, Giorgis D, Valloton A, Amelin Y (2000) U–Pb and Ar–Ar geochronoligical data from the Pelagonian Basement in Evia (Greece). Geodynamic implications for the evolution of Paleotethys. Schweisz Miner Petrog 80:21–43

Von Raumer JF, Stampfli GM (2008) The birth of the Rheic Ocean—Early Palaezoic subsidence patterns and tectonic plate scenarios. Tectonophysics 461:9–20

Von Raumer JF, Stampfli GM, Bussy F (2003) Gondwana-derived microcontinents—the constituents of the Variscan and Alpine collisional orogens. Tectonophysics 365:7–22

Von Raumer JF, Stampfli GM, Bussy F (2009) The Variscan evolution in the External massifs of the Alps and place in their Variscan framework. C R Geosci 341:239–252

Warr LN (2002) The Variscan orogeny: the welding of Pangea. In: Woodcock N, Strachan R (eds) Geological history of Britain and Ireland. Blackwell, Oxford, pp 271–294

West DP, Coish RA, Tomascak PB (2004) Tectonic setting and regional correlation of Ordovician metavolcanic rocks of the Casco Bay Group, Maine: evidence from trace element and isotope geochemistry. Geol Mag 141(2):125–140

Wilson M (1989) Igneous petrogenesis—a global tectonic approach. Chapman and Hall, London

Wood DA (1980) The application of a Th–Hf–Ta diagram to problems of tectonomagmatic classification and to establishing the nature of crustal contamination of basaltic lavas of the British Tertiary volcanic province. Earth Planet Sci Lett 50:11–30

Yaltırak C, Okay AI (2004) Edremit körfezi kuzeyinde Paleotetis birimlerinin jeolojisi. Bull Eng ITU 3(1):67–79

Yuan HL, Gao S, Liu XM (2004) Accurate U–Pb age and trace element determinations of zircon by laser ablation-inductively coupled plasma-mass spectrometry. Geostand Geoanal Res 28:353–370

Zanchi A, Garzanti E, Larghi C, Gaetani M (2003) The Variscan orogeny in Chios (Greece): carboniferous accretion along a Palaeotethyan active margin. Terra Nova 15:213–223

Ziegler P (1989) Evolution of Laurussia. Kluwer, Dordrecht